

# High-mobility 3D topological insulator nanoplatelets on hBN sheets

P. Gehring, B. Gao, M. Burghard, and K. Kern

Topological insulators (TIs) have attracted immense attention during the past few years due to the fact that they are insulators in the bulk, but manifest conducting helical states at their boundaries [1]. In contrast to the quantum Hall state, these boundary states originate from strong spin-orbit coupling without any external magnetic field, such that time reversal symmetry is conserved and accordingly backscattering is forbidden. The unique combination of dissipation-less charge transport channels with intrinsic spin polarization renders TIs of strong interest for spintronic applications. However, while theory predicts TIs to be perfect bulk insulators, their experimental charge transport behavior is dominated by point defects (e.g., Se vacancies). Such defects are commonly introduced during the growth of thin films of three-dimensional (3D) TIs such as  $\text{Bi}_2\text{Se}_3$ ,  $\text{Bi}_2\text{Te}_3$ , and  $\text{Sb}_2\text{Te}_3$ , which leads to strong bulk doping in these compounds. This leads to a quasi-metallic conduction channel parallel to the surface channels, rendering it difficult to unequivocally assign charge transport features to the topological protected surface states. Strategies to minimize the contribution of the bulk transport include compensation doping, alloying of differently doped TIs, or increasing the surface to bulk ratio by using ultrathin samples. However, doping or alloying often results in a drastic decrease in carrier mobility due to the introduction of structural defects. One promising strategy to improve the structural quality involves epitaxial growth of TI thin films on appropriate ultrathin crystal sheets. Thus far, epitaxial growth on graphene has been demonstrated to significantly reduce the defect density, although the electrically conductive graphene is not suitable as an underlying substrate if the grown TIs are to be characterized by charge transport experiments.

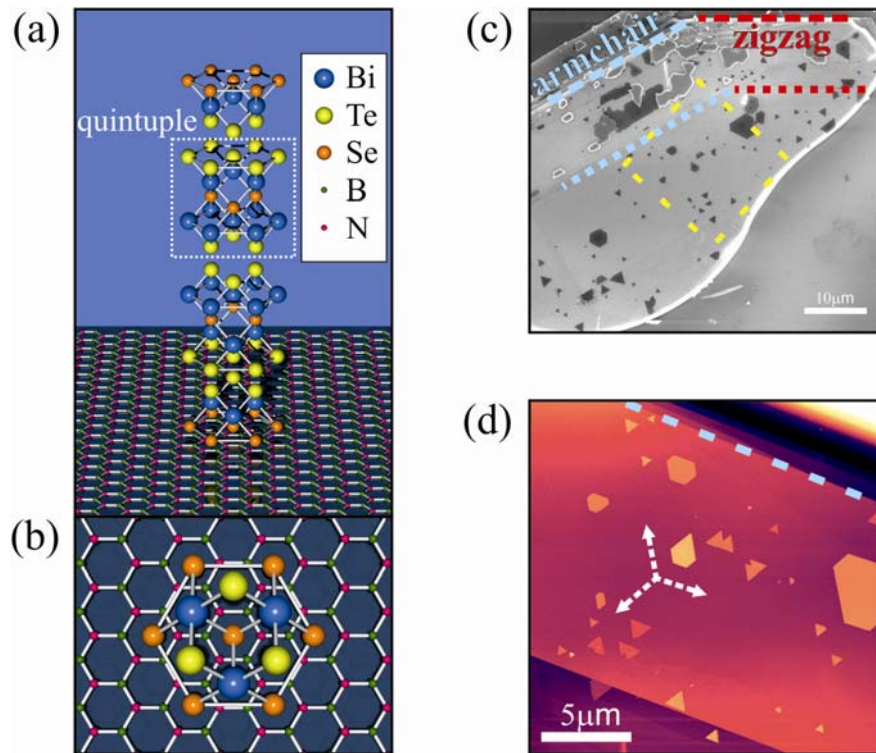


Figure 1: Van der Waals epitaxy of  $\text{Bi}_2\text{Te}_2\text{Se}$  on hexagonal boron nitride (hBN). Schematic illustration of (a) the crystal structure of  $\text{Bi}_2\text{Te}_2\text{Se}$ , and (b) the proposed epitaxial growth mode on hBN. Representative SEM (c) and AFM (d) image of  $\text{Bi}_2\text{Te}_2\text{Se}$  nanoplatelets grown on a hBN sheet. All platelets are oriented parallel or rotated by an angle of  $120^\circ$  (as indicated by the dashed arrows).

Here, we report the electrical properties of high quality  $\text{Bi}_2\text{Te}_2\text{Se}$  thin films obtained by van der Waals epitaxial growth on electrically insulating boron nitride sheets [2].  $\text{Bi}_2\text{Te}_2\text{Se}$  has emerged as one of the most prospective TIs due to its simple surface band structure, large bulk band gap and low bulk contribution to the total charge transport. It forms rhombohedral crystals consisting of

hexagonally close-packed atomic layers of five atoms (quintuple layer) arranged along the  $c$ -axis as follows:  $\text{Se}^{(1)}/\text{Te}^{(1)} - \text{Bi} - \text{Se}^{(2)}/\text{Te}^{(2)} - \text{Bi} - \text{Se}^{(1)}/\text{Te}^{(1)}$  (see Fig. 1(a)), with the lattice constants  $a = 4.283 \text{ \AA}$  and  $c = 29.846 \text{ \AA}$ . Hexagonal boron nitride (hBN), which likewise forms a layered crystal with hexagonal symmetry, has a lattice constant of  $1.45 \text{ \AA}$ , favoring a small lattice mismatch of 1.5% for  $\text{Bi}_2\text{Te}_2\text{Se}$  (Fig. 1(b)). The growth of thin  $\text{Bi}_2\text{Te}_2\text{Se}$  films was accomplished by a catalyst-free vapor-solid growth method, using hBN sheets prepared by micromechanical cleavage of hBN powder on  $\text{Si}/\text{SiO}_x$  substrates. The process yielded  $\text{Bi}_2\text{Te}_2\text{Se}$  films with a thickness between 10 and 500 nm, controllable by the position of the growth substrate within the furnace and the growth time. Microscopic inspection revealed that the  $\text{Bi}_2\text{Te}_2\text{Se}$  grows on top of the BN in the form of regular platelets with hexagonal symmetry (Fig. 1(c,d)). The crystal facets in all nanoplatelets are oriented either parallel or tilted by  $120^\circ$  or  $240^\circ$  with respect to each other, thus corroborating the epitaxial growth mode depicted in Fig. 1(b). This is further supported by the observation that the platelets preferably grow parallel to one of the sharp edges of the hBN sheet. As the edges of the hBN flake enclose an angle of precisely  $30^\circ$ , they can be assigned to armchair or zigzag edges. The edges marked in blue in Fig. 1(c) most likely represent the armchair rather than zigzag edges, because the resulting misfit would be unrealistically high in the zigzag case.

As distinguished from previously investigated  $\text{Bi}_2\text{Te}_2\text{Se}$  films deposited by vapor-solid growth on  $\text{Si}/\text{SiO}_x$  substrates, the present films display well-developed Shubnikov-de Haas (SdH) oscillations. They provide a means of testing the dimensionality of the charge transport in the samples. In Fig. 2(a), the high field part of the Hall resistance  $R_{xy}$  is plotted as a function of the magnetic field  $B$  for a 45 nm thick  $\text{Bi}_2\text{Te}_2\text{Se}$  platelet on a  $\sim 50$  nm thick hBN sheet ( $T = 1.5 \text{ K}$ ).

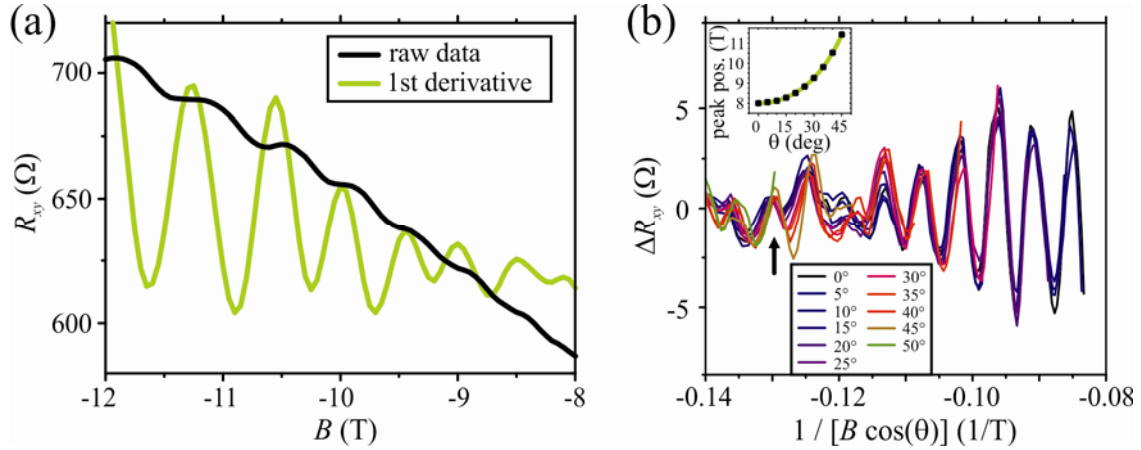


Figure 2: (a) Shubnikov-de-Haas (SdH) oscillations in the high-field Hall resistance as a function of the magnetic field (black curve); the green curve represents the first derivative. (b) Amplitude of the SdH oscillations as a function of  $1/(B \cdot \cos\theta)$  for different tilting angles  $\theta$  (between surface normal and magnetic field). The inset shows the position  $1/B$  of the SdH peak with the LL index  $n = 22$  (marked by the arrow) for different angles  $\theta$ , combined with a  $1/\cos\theta$  fit (green curve) to the data.

In a two-dimensional (2D) electron gas, SdH oscillations are periodic in  $1/B$ , with a periodicity given by

$$2\pi n = A_F \frac{\hbar}{eB},$$

where  $n$  is the Landau level (LL) index, and  $A_F$  is the external cross-section of the Fermi surface. As the LL formation is induced by the  $B$ -field component normal to the surface, the maxima/minima of the SdH oscillations should shift by  $1/(B \cdot \cos\theta)$  upon tilting the sample in the magnetic field  $B$ . Figure 2(b) shows that in the plot of the SdH oscillation amplitude vs. the perpendicular  $B$ -field component indeed all curves coincide up to an angle of  $50^\circ$ . That the SdH oscillations originate from the topological 2D surface states is further underscored by the smooth fit of the dependence of the position of a selected peak on the tilting angle  $\theta$  by a  $1/\cos(\theta)$  function (see inset of Fig. 2(b)).

In order to determine the carrier mobility, we performed Hall measurements on thin  $\text{Bi}_2\text{Te}_2\text{Se}$  films that permit tuning of the Fermi level through the action of a back gate. Figure 3(a) presents Hall data gained from the sample described above. All curves show negative slopes up to the highest negative gate voltages, indicating an n-doping character. The pronounced nonlinearity of the curves points toward the contribution of two transport channels to the total electrical transport. Fitting the curves by a two-band model comprising parallel conduction of bulk and surface carriers yielded the corresponding mobility as a function of gate voltage (Fig. 3(b)). It is apparent that the mobility of the topological surface state is one to two orders of magnitude higher than the bulk value over the entire gate voltage range. The impressive surface state carrier mobility in the range of 8.000 to 20.000  $\text{cm}^2/\text{Vs}$  is attributable to the reduced defect density in the films grown by van der Waals epitaxy, a conclusion that gains support by comparing  $\text{Bi}_2\text{Te}_2\text{Se}$  thin films grown on hBN vs.  $\text{Si}/\text{SiO}_x$  substrates. Specifically, for  $\text{Bi}_2\text{Te}_2\text{Se}$  on hBN the average surface state mobility was found to be  $\sim 4.900 \text{ cm}^2/\text{Vs}$ , approximately three times larger than the value of  $1.600 \text{ cm}^2/\text{Vs}$  obtained in case of the  $\text{Si}/\text{SiO}_x$  substrates. Furthermore, Fig. 3(b) evidences that upon lowering the electron density, the surface carrier mobility first increases, and then decreases again. While the initial mobility increase may be due to reduced electron-electron (Coulomb) interactions, the subsequent decrease could originate from the opening of new scattering channel from the surface states into the bulk VB when the Fermi level position approaches the valence band (VB) edge, which in  $\text{Bi}_2\text{Te}_2\text{Se}$  is located above the charge neutrality (Dirac) point. A similar scenario has recently been put forward to explain scattering effects observed in scanning tunneling microscopy on the closely related TI  $\text{Bi}_2\text{Se}_3$ .

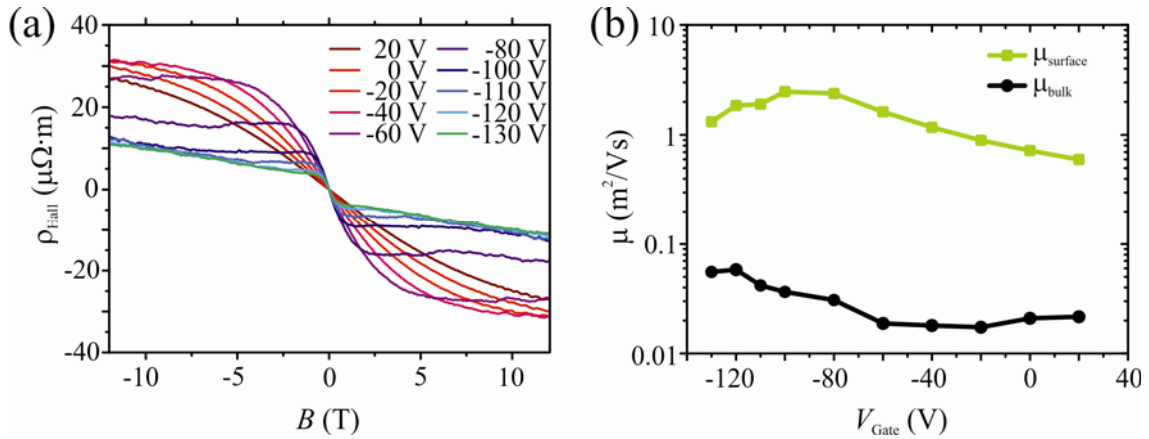


Figure 3: Hall measurements of epitaxially grown  $\text{Bi}_2\text{Te}_2\text{Se}$  films on hBN, performed at  $T = 1.5 \text{ K}$ . (a) Hall resistivity as a function of  $B$ -field for different back gate voltages. (b) Comparison of the bulk (black curve) and surface state (green curve) mobility for different gate voltages, as obtained using the two-band model fit.

The gate-dependent mobility values derived from the Hall measurements were found to be in good agreement with those extracted from the SdH oscillations. Interestingly, only a single SdH oscillation period could be observed for all gate voltages, indicating the contribution of only one surface state. A similar conclusion has recently been drawn from magnetotransport experiments on  $\text{Bi}_2\text{Te}_2\text{Se}$  nanoplatelets grown directly on  $\text{Si}/\text{SiO}_x$  [3]. One possible explanation is a chemical surface reaction taking place upon prolonged air exposure which deactivates the top surface state of the platelets (while the bottom surface close to the hBN remains well protected). At the present stage, only little is known about the surface chemistry of TIs in general. Future studies are hence desired to explore the influence of the chemical environment on the composition and atomic structure of different TI surfaces.

#### References:

- [1] Yan, B. and S.-C. Zhang. Rep. Prog. Phys. **75**, 096501 (2012).
- [2] Gehring, P., B. Gao, M. Burghard, and K. Kern. Nano Letters **12**, 5137-5142 (2012).
- [3] Gehring, P., B. Gao, M. Burghard, and K. Kern. Appl. Phys. Lett. **101**, 023116 (2012).

#### In collaboration with:

B. Gao (Shanghai Institute of Microsystem and Information Technology, China)